



International Commission on Illumination
Commission Internationale de l'Eclairage
Internationale Beleuchtungskommission

ASSESSMENT OF THE VALIDITY OF THE CURRENT MINIMAL TEST DISTANCES OF (O)LED LUMINAIRES

Dotreppe, G.M., et al.

DOI 10.25039/x051.2025/66v4jy

This article is also published as part of:

Proceedings of the CIE 2025 Midterm Meeting Vienna, Austria, July 4-11, 2025:
Scientific Conference (July 7-9, 2025)

DOI 10.25039/x051.2025

in

Proceedings of the CIE (International Commission on Illumination)

ISSN no. 3061-015X (print), 3061-0168 (online)

The paper has undergone double-blind peer review and its final version has been presented at the CIE 2025 Midterm Meeting, Vienna, Austria, July 4–11, 2025.

© CIE 2025

All rights reserved. This work is licensed under the Creative Commons Attribution-NonCommercial 4.0 International License (<https://creativecommons.org/licenses/by-nc/4.0/>). Any mention of organizations or products does not imply endorsement by the CIE.

CIE Central Bureau
Babenbergerstrasse 9/9A
A-1010 Vienna, Austria
Tel.: +43 1 714 31 87
e-mail: ciecb@cie.co.at — www.cie.co.at

ASSESSMENT OF THE VALIDITY OF THE CURRENT MINIMAL TEST DISTANCES OF (O)LED LUMINAIRES

Dotreppe, G.M.¹, Van den Bossche, P.¹ Jacobs, V.A.¹

¹ Vrije Universiteit Brussel — Merlin at MOBI research group, Brussels, Belgium;
valery.ann.jacobs@vub.be

Abstract

Standardisation bodies including the CIE and IESNA propose several test distances for far-field photometry based on the applicability of the inverse square law. Depending on the beam width, luminaire size and configuration, various guidelines regarding the minimal test distance are proposed. Recent literature suggests some norms are overoptimistic and larger far-field distances are required. Furthermore, the proposed test distances are only based on observations along the optical axis, whereas a strong angular variation of the limiting photometric distance was recently demonstrated. Therefore, this work presents a comparison between the regulations and the observations made in recent literature, assessing the application region of the standardised test distances as a function of the luminaire characteristics and the location of the measurement equipment.

Keywords: Photometry, Far-Field, Near-Field, LED, OLED, Photometric Distance

1 Introduction

Light sources are typically characterised by a Luminous Intensity Distribution (LID), applicable when the source can be approximated as a radiating point. This is a valid assumption beyond a certain distance, known as the Limiting Photometric Distance (LPD) (Liu et al., 2013, Simonas and Bean, 2001, Dotreppe et al., 2023). Along the optical axis, the LPD has been determined mainly experimentally or using analytical solutions for the radiative transfer function (RTF). Standards such as CIE S025/E:2015 suggest test distances based on source geometry and beam pattern (CIE, 2015), while CIE 43 provides stricter guidelines for floodlights with limited Full Width Half Maximum (FWHM) (CIE, 1979). In contrast, IES LM 79-2019 recommends a minimum test distance of five times the source's largest dimension for near Lambertian distributions, with experimental verification advised for other sources (ANSI/IES, 2019). Similarly, IEC/TR 61341 prescribes constant test distances regardless of beam shape (IEC, 2010). However, as shown by Bergen and Jenkins (2012), these guidelines often fail for modern LED based systems. Therefore, the authors proposed a modified floodlight rule, accounting for non-luminous spaces. This equation solely needs the physical source geometry and FWHM rendering it practical for photometric studies. In contrast to previous standards, this rule, applicable to all distributions following a power cosine, considers both the luminous and non-luminous areas of a luminaire, a result later confirmed by Jacobs et al (2014).

Despite these advancements, recent research has observed that even these updated guidelines might fall short. Moreno and Sun (2008) demonstrated that the LPD depends on LED packing density and beam patterns, noting reduced LPDs for denser packaging and wider FWHM. Furthermore, it was inferred that side emitters and Batwing distributions showed a smaller on-axis LPD distance compared to Lambertians. Their subsequent study proposed using weighted root mean square (RMS) errors across angular distributions for the LPD assessment, which adjusted previous results, now showing higher LPDs for Batwing distributions compared to Lambertians (Moreno et al., 2009). Cai et al. (2013) refined this by scaling RMS errors with the sum of the far-field intensity over the complete angular range instead of the peak intensity. Their findings highlight this method's sensitivity, ranking the LPD for Lambertian sources as the lowest, followed by side emitters, narrow beams, and Batwings. Sun et al. (2009) employed the Normalised Cross Correlation (NCC) to identify the far-field region. This method, however, was observed to be less sensitive and too conservative (Cai et al., 2013). In Sun et al. (2020) the maximal LPD value of an array of LEDs is computed using a point source assumption, considering the source as an extended flat surface and through a ray tracing simulation. Depending on the array configuration (hollow or full) and the source representation, varying LPD estimations are observed. In contradiction to the above studies, the luminaire is shown to

obey at most the five times rule. While scarce, several theoretical computations of the LPD have been performed. Jacobs et al. (2015) demonstrated much longer far-field distances for narrow-beam circular sources in comparison to the standards published at that time. Similarly, Liu et al. (2013) computed the LPD by solving the RTF for various luminaire geometries assuming a Lambertian distribution. While limited in applicability, the study demonstrated the increase in LPD as the non-luminous area increases.

Despite extensive research, inconsistencies persist due to oversight of luminaire geometry or angular LPD variation. To address this, Dotreppe et al. (2023) used a numerical model validated against ray tracing simulations and direct illuminance measurements to assess the illuminance at an arbitrary location in space. Findings reveal significant angular LPD dependence, challenging current standard test distances, which are predominantly computed along the optical axis. Off-axis values frequently exceed minimal test distances, questioning the validity of LID measurement and inverse square law application for illuminance calculations.

2 Materials and Methods

2.1 Devices under test

In a first instance, four devices under test (DUTs) are considered: (a) a single Lambertian source, (b) a narrow-beam LED with a FWHM of 18°, and an array of (c) two Lambertian sources and (d) two such narrow-beam LEDs separated by a non-luminous area of 10 times the individual LED’s diameter. The DUTs are respectively referred to as DUT 1, 2, 3 and 4. For the ease of comparison, all light sources will have identical dimensions and a uniform luminance distribution across their surface. The characteristic dimension (CD) of the luminaires comprised of a single source is defined as their largest luminous dimension, i.e. their diameter. For the arrays, this translates to the sum of the non-luminous separation and the largest luminous dimension of the luminaire in accordance with CIE S 025 (CIE, 2015). Lambertians are modelled using a single cosine luminance model, while the narrow-beam DUTs use the dual cosine model. The individual sources comprising the arrays are aligned with the C0/180 plane. The luminous areas and the non-luminous spacings are kept identical for all DUTs. Finally, a unit peak far-field intensity is assumed.

Later, this study will analyse the influence of the beam width of the luminaire, the considered C-plane, and the non-luminous separation. As parametrising the dual cosine model based on a beam width proves cumbersome, each source is modelled using a single power cosine. The individual sources have identical dimensions.

2.2 Photometric computations

This study will compare the LPD estimations proposed in literature and standards for a variety of light sources. To assess the LPD, the illuminance (or apparent intensity I_{app}) values anywhere in space are required so that the relative error with far-field quantities can be computed. A numerical approach is used to assess the illuminance in the near-field, retaining the extended nature of the light source, and far-field where the light source is represented as a radiating point. To this end, the luminous surface is discretised, assigning each infinitesimal surface element a rotationally symmetric luminance distribution following either a single (L_s) or dual (L_d) power cosine as:

$$L_s(\mathbf{r}_s, \gamma) = L_0 \cos^{n1} \gamma \tag{1}$$

$$L_d(\mathbf{r}_s, \gamma) = L_{01} \cos^{n1} \gamma + L_{02} \cos^{n2} \gamma \tag{2}$$

where

- n determines the half FWHM;
- γ is the emission angle;
- L_0 is the Luminance along the optical axis;
- \mathbf{r}_s location of the emitting surface element on the extended light source.

The RTF is approximated through a Riemann sum of the contribution of each luminous surface element. The dual cosine model is used for sources exhibiting a more gradual decrease of the luminance at extreme emission angles.

The numerical approach was validated through ray-tracing simulations and direct illuminance measurements on a variety of sources. For illustrative purposes, Figure 1 shows the validation for an array of two narrow-beam LEDs at 3 distances corresponding to 2, 5 and 10 times the separation of the LEDs. The plane displayed is the C0/180 plane, defined as the plane connecting both LEDs. A good agreement is observed between all computation methods and the measurements. The dual cosine better represents the distribution tails and will therefore be used for this DUT. Other narrow beams are modelled through a single cosine due to the straightforward link between the cosine power and the half FWHM.

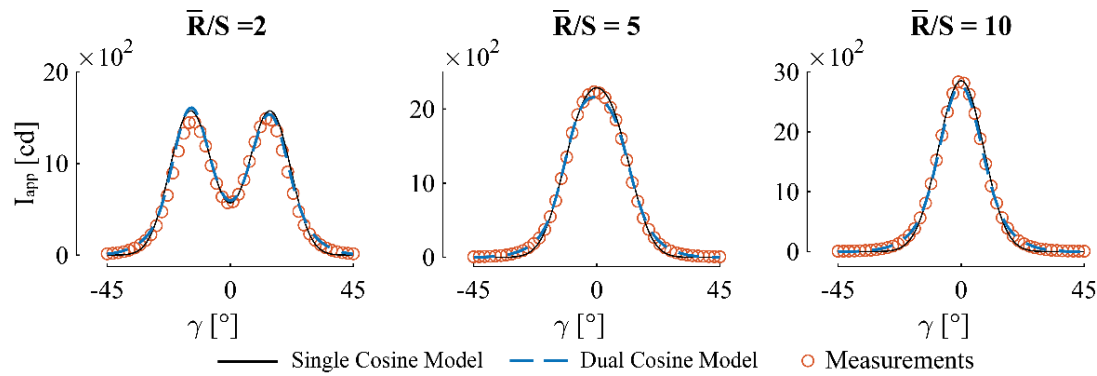


Figure 1 – Angular intensity distribution of a two-LED narrow-beam array (C0/180 plane only), comparing three measurement distances. Results from a single and dual cosine-based numeric model are compared with physical measurements. Good agreement is observed across all distances.

For the dual LED arrays, the computations are limited to the C0/180 and C90/270 plane, because these represent the most extreme cases for this luminaire configuration. The remaining C-planes exhibit intermediate characteristics that fall between these two extremes.

2.3 LPD estimation

The LPD is estimated using the criteria described in section 1, summarised in Table 1. To analyse their validity, an LPD estimation can be made for arbitrary emission angles γ and C-planes as the post-ultimate distance with a relative error between the apparent and far-field intensity larger than 1%:

$$\forall \gamma, \forall C: \exists LPD(\gamma, C) | \forall \bar{R} \geq LPD: \epsilon(\bar{R}, \gamma, C) = \left(1 - \frac{I_{app}(\bar{R}, \gamma, C)}{I_{FF}(\gamma, C)} \right) \times 100\% \leq 1\% \quad (3)$$

This location is chosen to avoid false LPD assessments due to local maxima observed in the apparent intensity profiles as shown in Dotreppe et al. (2023). Note that this approach assumes a fixed point source located in the geometric centre of the luminaire.

Table 1 – Summary of the LPD rules discussed.

CIE S 025 (CIE, 2015)	
For DUT having near cosine distribution (beam angle $\geq 90^\circ$) in all C-planes	$LPD \geq 5 \times D$
For DUT having a broad angular distribution different from a cosine distribution (beam angle $\geq 60^\circ$) in some of the C-planes	$LPD \geq 10 \times D$
For DUT with narrower angular distributions, steep gradients in the luminous intensity distribution or critical glare control	$LPD \geq 15 \times D$
For DUT where there are large non-luminous spaces between the luminous areas	$LPD \geq 15 \times (D + S)$

CIE 43 (CIE, 1979):	$LPD > D \frac{200}{FWHM}$
Modified Floodlight Rule (Bergen and Jenkins, 2012):	$LPD > (D + S) \frac{200}{FWHM}$
Moreno et al. (2009):	$RMS_{I_{Max}} = \sqrt{\frac{1}{M} \sum_{i=1}^M \frac{I(\gamma_i, C_i)}{I(\gamma_i, C_i)_{Max}} \left[\frac{I_{app}(\gamma_i, C_i)}{I(\gamma_i, C_i)} - 1 \right]^2} \leq 0.0055$
Cai et al. (2013) :	$RMS_{I_{Sum}} = \sqrt{\sum_{i=1}^M \frac{I(\gamma_i, C_i)}{\sum I(\gamma_i, C_i)} \left[\frac{I_{app}(\gamma_i, C_i)}{I(\gamma_i, C_i)} - 1 \right]^2} \leq 0.01$
Sun et al. (2009) :	$NCC = \frac{\sum_i [I_{app}(\gamma_i, C_i) - \bar{I}_{app}] [I(\gamma_i, C_i) - \bar{I}]}{\sqrt{\sum_i [I_{app}(\gamma_i, C_i) - \bar{I}_{app}]^2 \sum_i [I(\gamma_i, C_i) - \bar{I}]^2}} \geq 99.9$

i represents the amount of considered sources in a multi-source luminaire. $I_{app}(\gamma, C)$ is the apparent intensity for a certain γ -angle and C-plane. $I(\gamma_i, C_i)$ is the far-field intensity and $I(\gamma_i, C_i)^{Max}$ is its maximum value. Overbars represent the distribution mean over the angular range. D is the largest luminous dimension, and S is the non-luminous separation.

3 Results

3.1 LPD comparison for the DUTs

The angular distribution of the LPD for the four DUTs is shown in Figure 2. Lambertian sources are modelled through a single cosine luminance model using Eq. (1), while the narrow beams use the dual cosine model from Eq. (2). A strong variation of the LPD is observed, with values surpassing the on-axis LPD in many cases, especially for the luminaires comprised of separated LEDs. This prompts the investigation of the validity of current standard LID test distances. Table 2 summarises the LPD for the DUTs, expressed as a multiple of their characteristic dimension, with the highest values highlighted. The reported LPDs vary significantly depending on the estimation method, the FWHM of the source, and the presence of non-luminous areas. These three aspects play a critical role in the applicability of the recommended test distances.

The CIE S 025 standard proves insufficient, as it fails to account explicitly for the FWHM of LED and arrays thereof. For DUT 2 and 4 it produces shorter LPD values compared to various alternative LPD estimations. Inversely, due to the lack of consideration of the source’s FWHM, the LPD for DUT 3 is largely overestimated compared to other metrics. Similarly, CIE 43 is clearly unsuitable for broad distributions, systematically underestimating the minimum measurement distance. Furthermore, it yields identical values regardless of the presence of non-luminous areas, which is unrealistic. The modified floodlight rule addresses this omission of non-luminous areas, providing improved LPD estimates. However, it can also result in very large LPD distances, as in the case of DUT 4, where it largely exceeds the next biggest LPD found in the off-axis direction at the luminaire's FWHM. The on-axis LPD derived from the relative error between apparent and far-field intensity provides a reliable estimation along the optical axis, aligning well with the analytically derived value for a single Lambertian source. Nonetheless, it remains limited to a single direction and may not accurately represent the LPD across the entire distribution. That said, if the on-axis LPD is not respected, the peak intensity measurement becomes unreliable. This metric can therefore be considered a first order estimate for the minimum test distance.

Metrics based on the complete luminous distribution tend to be more conservative than their on-axis counterparts for single-source luminaires, whereas the opposite may hold for dual-source configurations depending on the FWHM. The $RMS_{I_{Max}}$ criterion tends to favour single-source designs, whereas $RMS_{I_{Sum}}$ is more restrictive for arrays. It shall be noted that this strongly depends on the threshold value. Moreno et al. (2009) used the error obtained at $5 \times D$ for a circular Lambertian source to obtain a limit value. Cai et al. (2013) arbitrarily chose a limit value of 1%. The LPD for DUT 1 demonstrates that this threshold is too large, as the theoretical valid LPD for a Lambertian is underestimated. Hence, to obtain a threshold value resulting in comparable LPDs, the approach proposed by Moreno et al. (2009) is applied to the $RMS_{I_{Sum}}$,

resulting in a threshold value of 0.0069 used from now on. The *NCC* method, by contrast, performs poorly across all tested configurations and is not recommended.

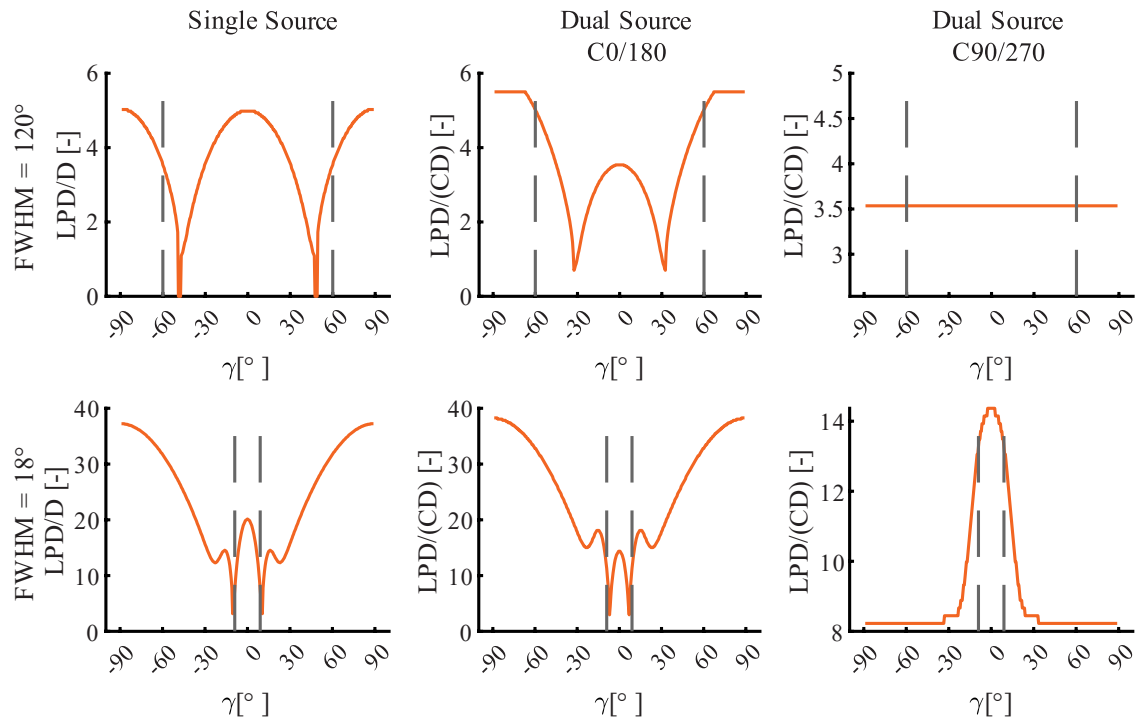


Figure 2 – LPD distribution for the 4 DUTs as a function of the emission angle. The dashed lines represent the FWHM boundaries of the respective luminaires.

Table 2 – LPD for the DUTs using methods described in the latest standards and literature. Values are given as a multiple of the characteristic dimension of the DUT.

		DUT 1 1 LED FWHM = 120°	DUT 2 1 LED FWHM = 18°	DUT 3 2 LEDs FWHM = 120°	DUT 4 2 LEDs FWHM = 18°
On-Axis	CIE S 025 (CIE, 2015)	5.0	15.0	15.0	15.0
	CIE 43 (CIE, 1979)	3.3	22.0	1.8	12.1
	Modified floodlight (Bergen and Jenkins, 2012)	3.3	22.0	3.3	22.0
	$\epsilon_{On-Axis} < 1\%$ (Moreno and Sun, 2008, Liu et al., 2013)	5.0	20.0	3.5	14.4
Full Distribution	$RMS_{I_{max}} < 0.0055$ (Moreno et al., 2009)	5.0	13.3	4.8	10.7
	$RMS_{I_{sum}} < 0.01$ (Cai et al., 2013)	4.1	16.7	4.0	13.7
	$NCC > 99.9$ (Sun et al., 2009)	2.1	6.0	2.2	5.8
	Off-Axis at FWHM/2 (as per Eq. (3))	4.0	6.4	5.0	17.0

Finally, the off-axis LPD evaluated at the FWHM angle yields the second-highest values for narrow beams, surpassing the on-axis LPD. This underscores the importance of considering directions beyond the optical axis for LPD estimations. However, for single source luminaires (DUT 1 and 2) it underestimates the LPD compared to alternative estimation methods. Hence, a deeper dive into the different metrics based on the three considered luminaire characteristics is required.

The validity of the existing LPD criteria is further analysed by comparing them with the LPD computed through Eq. (3) along the optical axis, at the half FWHM and at the half Full Width at Tenth Maximum (FWTM) for a range of luminaires. The latter is introduced as a considerable amount of illumination is still expected in directions with 10% of the peak intensity, its LPD is generally located further than along the optical axis, as can be deduced from Figure 2. The considered luminaires have a beam width from 10° to 120°, with a separation between 0 and

$100 \times CD$. Three cases are considered: case 1 where a single source shows a variable FWHM, case 2 studying an array with fixed separation but variable FWHM, and case 3 where the array has a fixed FWHM, but a varying separation.

3.2 Case 1: Single source

Figure 3(a) shows the simulation results for a single source with variable FWHM modelled through Eq. (1). The LPD obtained through the $RMS_{I_{Max}}$ and $RMS_{I_{Sum}}$ are shown as a dashed and dotted line respectively. For the $RMS_{I_{Max}}$, the threshold value of 0.0055 is kept, but the new threshold value of 0.0069 is used for the $RMS_{I_{Sum}}$ based on the theoretical LPD of $5 \times D$ for a Lambertian source. For the assessment of the validity of standard measurement distances, a reference distance resulting in the lowest possible measurement error due to the distance setting is to be chosen. The LPD at FWTM proves to be always larger than along the optical axis and at the FWHM, rendering it as a good candidate. The $RMS_{I_{Sum}}$ is more sensitive than the $RMS_{I_{Max}}$, laying in between the on-axis LPD estimations and the one at the FWTM. Because the $RMS_{I_{Sum}}$ takes the full distribution into account, considering both peak and small intensity values within a single metric, this LPD is used as reference distance.

The LPD as computed through the $RMS_{I_{Sum}}$ is compared to standardised measurement distances proposed in CIE S 025/E:2015 and CIE 43 in Figure 3(b) (CIE, 2015, CIE, 1979). The modified floodlight rule is not presented as it reduces to the floodlight rule of CIE 43 for single light sources ($S = 0$). The CIE S 025 shows three reference values depending only on the FWHM angle. It is valid for a FWHM of 120° but underestimates the LPD for angles between 90° and 120° . For FWHM angles between 26° and 90° , a strong overestimation of the distance is observed, followed again by an underestimation for beam angles $\leq 26^\circ$. Hence, while often overestimated, the reference distances provided are valid for an FWHM range of 26° to 90° . CIE 43 follows a continuous curve as a function of the FWHM angle, only reaching the LPD bound for a beam angle smaller 32° .

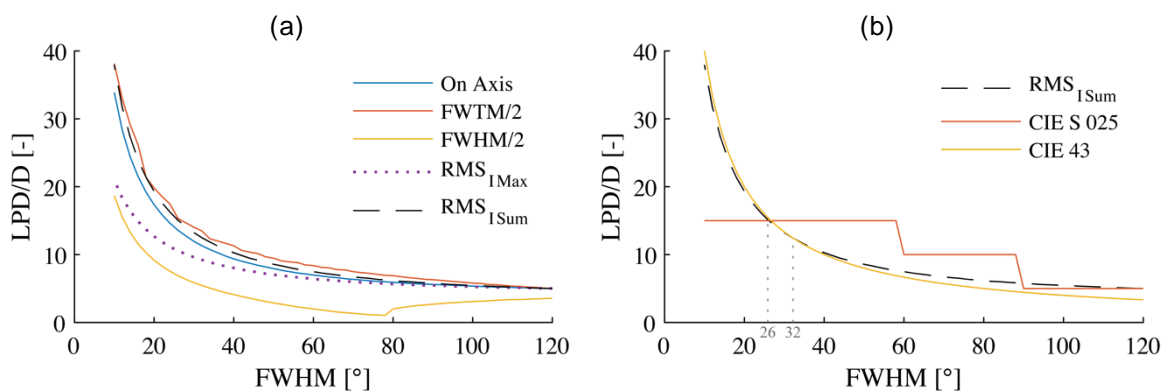


Figure 3 – LPD computations for light sources with variable FWHM. (a) shows the different LPD computations and (b) the comparison between the chosen reference LPD and the existing standards.

3.3 Case 2: Dual source; same separation, different FWHM

For the light source arrays, two C-planes are analysed. Figure 4(a) shows the computed LPDs for the C0/180 plane, and Figure 4(c) the ones for the C90/270 plane. The C0/180 plane shows a large variation in the LPD assessed for different emission angles. Contrary to the single light source, the on-axis LPD is not always larger than the LPD at the half FWHM. The latter suggests a larger LPD for sources with a beam $\geq 63^\circ$. Nevertheless, the LPD at the half FWTM is always the largest. The metrics considering the complete distribution show an in-between behaviour, with the $RMS_{I_{Max}}$ presenting larger distances for all beam angles compare to the $RMS_{I_{Sum}}$. Hence, the metric proposed by Cai et al. (2013) will again be used as reference value.

In the C90/270 plane, the LPD values estimated along the optical axis, at the half FWHM and at the half FTWM all reduce to the same value. This is due to the equal contribution of both

sources to the captured optical flux in this plane. The LPD computed through the $RMS_{I_{Sum}}$ suggests the largest LPD for all beam angles and will therefore be used as reference value.

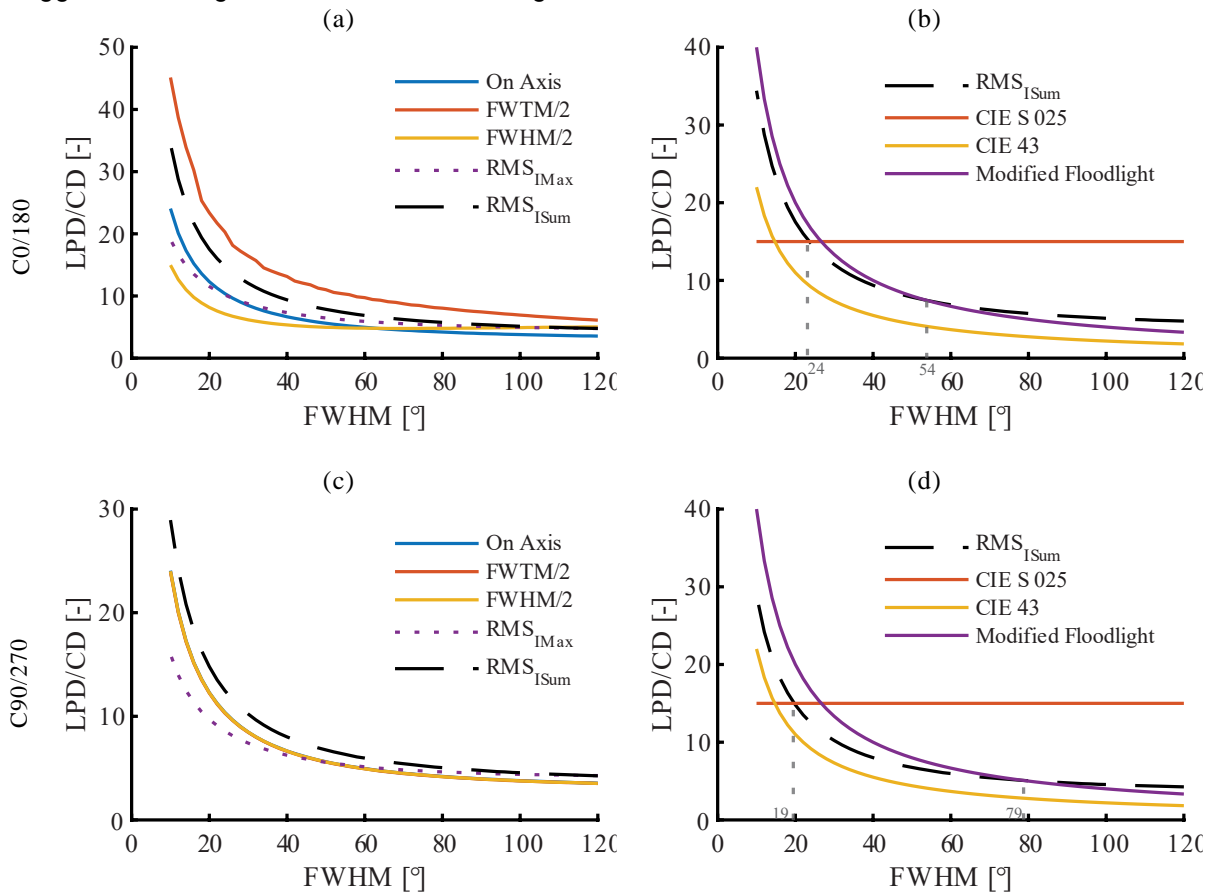


Figure 4 – LPD computations for an array of two LEDs with variable FWHM in (a) the C0/180 plane and (c) the C90/270 plane. (b) and (d) show a comparison between the chosen reference LPD and the existing standards.

Figures 4(b) and (d) show the standardised LPDs against the chosen reference value for the C0/180 and C90/270 plane respectively. In the former, the LPD suggested by CIE 43 is always strongly underestimated compared to the $RMS_{I_{Sum}}$ based computations. The CIE S 025 suggests a constant LPD, omitting the influence of the FWHM. The suggested measurement distance is larger than the computed one for luminaires with a beam angle $\geq 24^\circ$. The modified floodlight rule aligns better with the reference LPD, though it underestimates slightly for beam angles $\leq 54^\circ$, and then overestimates the LPD. Similar observations are made in the C90/270 plane. Here the CIE S 025 overestimates the LPD for beam angles $\geq 19^\circ$, while the modified floodlight rule underestimates the LPD for beam angles $\geq 79^\circ$. Table 3 summarises these results as a valid FWHM application region for the considered standard test distances.

Table 3 – Summary of the FWHM application region of the standard test distances.

Standard	Single Source	C0/180	C90/270
CIE S 025 (CIE,2015)	[26°; 90°] & 120°	$\geq 24^\circ$	$\geq 19^\circ$
CIE 43 (CIE, 1979)	$\leq 32^\circ$	N/A	N/A
Modified Floodlight Rule (Bergen and Jenkins, 2012)	$\leq 32^\circ$	$\leq 54^\circ$	$\leq 79^\circ$

3.4 Case 3: Dual source; different separation, same FWHM

Figures 5(a) and (c) show the absolute LPD as a function of the luminaire separation computed through Eq. (3) along the optical axis, at the half FWHM and at the half FWTM for the C0/180 and C90/270 plane respectively. The luminaire considered in this example has a beam width of 18° and source diameters of 15 mm. The LPD profiles show a linear increase for all computation methods. The LPD estimation is the largest along the FWTM angle, followed by the on-axis estimation and then at the FWHM. The metric proposed by Cai et al. (2013), based on the $RMS_{I_{Sum}}$, showed a value in between the ones computed along the optical axis and the one at the FWTM. In the C90/270 plane, the LPD computations at dedicated angles are all nearly identical due to the equal contribution of the individual light sources to the total captured optical power. The LPD computed through Eq. (3) for any angle lays in between the one estimated through the $RMS_{I_{Sum}}$ and $RMS_{I_{Max}}$. As the $RMS_{I_{Sum}}$ uses the complete distribution, hence considering both peak and small intensity values, this will be used as reference value to compare the validity of existing norms both in the C0/180 and C90/270 planes.

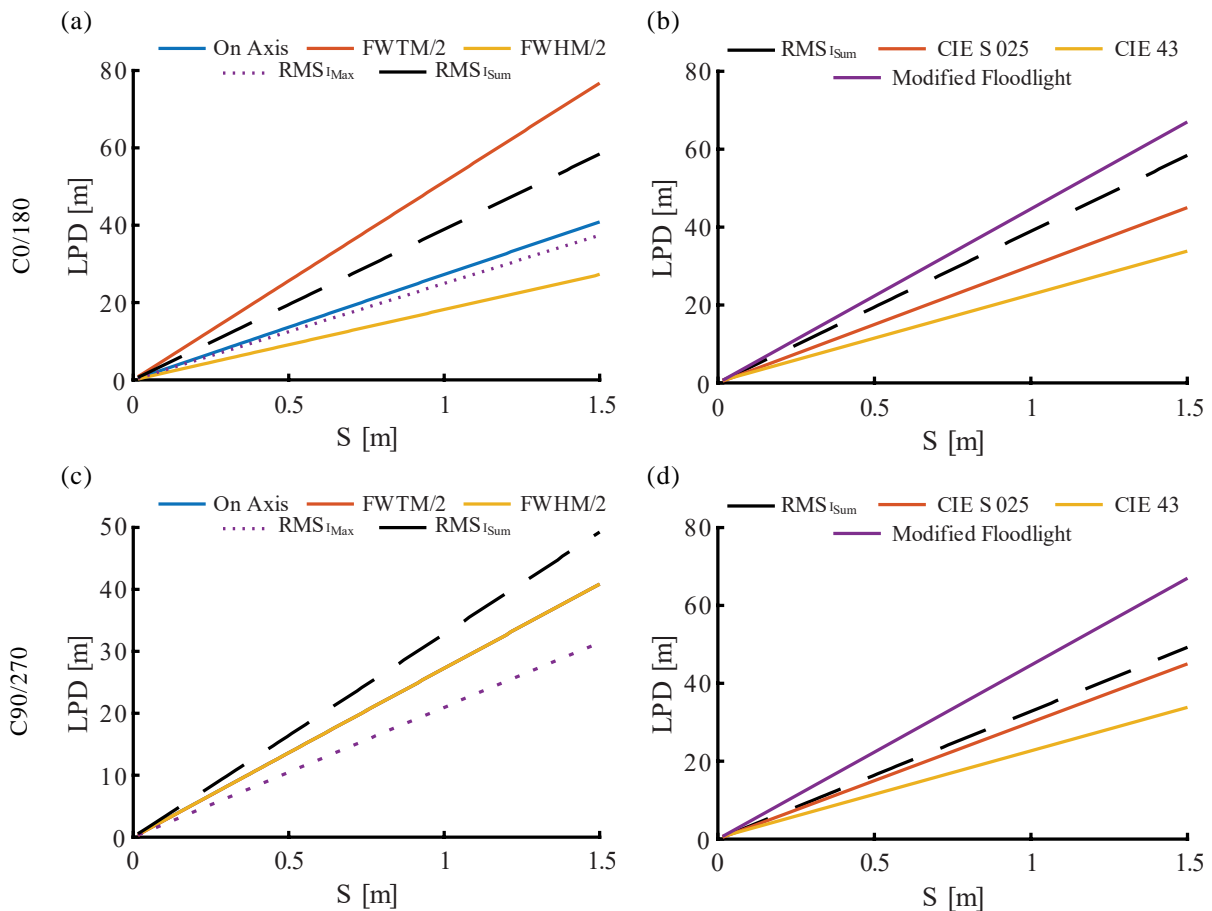


Figure 5 – LPD computations for an array of two LEDs ($FWHM = 18^\circ$, $D_i = 0.015$ m) with variable separation in (a) the C0/180 plane and (c) the C90/270 plane. (b) and (d) show a comparison between the chosen reference LPD and the existing standards.

Figures 5(b) and (d) show the comparison between the LPD computed through the $RMS_{I_{Sum}}$ and the standardised values proposed by CIE 43, CIE S 025 and the modified floodlight rule. Identical conclusions can be drawn irrespective of the observed plane. The modified floodlight rule provides measurement distances significantly higher than the one suggested by the reference computations. Inversely, CIE S 025 and CIE 43 underestimate the required measurement distance. Note that these observations are made for a luminaire having a beam width of 18°. As illustrated in Figure 4(b), the modified floodlight rule is valid for luminaires having a beam width smaller than 54°, while for the CIE S 025, the beam width needs to be larger than 24°. It can thus be inferred, that if the beam width is within the FWHM application region of the considered standard, it will present valid measurement distances for any source separation.

4 Discussion

The results indicate that the applicability of current standard test distances is highly dependent on three factors: the FWHM of the luminaire, the presence of non-luminous spacing between individual sources, and the overall luminous extent of the source.

While CIE S 025 recommends measurement distances that are sufficient for single-source luminaires with FWHM values between 26° and 90°, and at 120°, notable shortcomings arise elsewhere. Distances between 90° and 120° are systematically underestimated, and below 26°, the underestimation becomes severe. Such discrepancies suggest that CIE S 025, although robust within a limited parameter space, lacks adaptability for narrower beams. Similarly, for multi-source luminaires, the standard distances based solely on luminous area and source separation remain valid only for luminaires with beam angles above 24°. Below this threshold, significant measurement errors emerge, undermining the reliability of the method for arrays of narrow beams.

CIE 43 exhibits comparable limitations. It is applicable for single-source luminaires with beam angles under 32° but underestimates the necessary distances for broader beams. Moreover, for arrays of light sources, the failure of CIE 43 to account for the non-luminous separation between individual emitters leads to consistently insufficient distances, irrespective of the source's separation. Although Bergen et al. (2012) propose a modification to the floodlight rule to address this, its validity remains confined to luminaires with beam angles up to 54°, thereby offering only a partial solution.

These findings underscore the absence of a universally applicable metric across the full diversity of luminaire designs. Existing standards exhibit substantial gaps, particularly for narrow-beam sources and arrays thereof. This reflects a broader issue: the difficulty of developing a single criterion that sufficiently encapsulates the complex interplay between source geometry, beam distribution, and spacing effects.

To address these limitations, two approaches are proposed. First, a data-driven metric derived from a curve fitting to a broad range of luminaire characteristics, including non-luminous separation, FWHM, and luminous area, could offer improved generalisability. Second, the construction of a detailed reference table, similarly grounded in these key parameters, may provide a practical tool for practitioners while retaining sufficient accuracy across a wide range of configurations. Alternatively, the modified floodlight rule can be made more stringent by adding an offset value, expanding its validity region to luminaires with broader distributions. However, this needlessly increases the test distance for narrower beams.

Note that the presented results are limited to a single cosine luminance model, assuming a uniform luminance distribution and a fixed location for the (geometric) photometric centre*. Sources using focussing optics will exhibit non uniformities in the luminance distribution and a projection of their centre of gravity which changes depending on the observation angle. The former proves to be less of an issue for the considered measurement distances (Dotreppe et al., 2023). The latter has fundamental implications on the LPD estimations but is difficult to consider for the definition of practical measurement distances. This aspect can only be assessed through empirical means. These are complicated to carry out for a wide range of luminaires and emission angles, requiring specialised measurement infrastructure and considerable time investments. We believe that at sufficiently large measurement distances, the influence of variations in the projected centre of gravity becomes negligible for the LID measurement. Nevertheless, a more in-depth analysis of this effect is required to confirm the above assumption and validate the findings presented through a numerical simulation.

Furthermore, it would be interesting to assess the measurement errors induced in various location when the suggested measurement distances computed through the $RMS_{I_{MAX}}$ are not respected. Depending on the requirements, shorter measurement distances could be acceptable.

* See CIE 121-1996 (CIE, 1996) or <https://cie.co.at/eilvterm/17-25-103>

5 Conclusions

Through this work, the applicability of current standards regarding the minimal measurement distance for far-field goniophotometric measurements is analysed. Based on numeric photometric computations, the LPD can be computed in all directions for a variety of luminaire configurations. Current results show that the latest standards are not always stringent enough to encompass the narrow beams and more complex luminaire compositions used nowadays and this due to the lack of consideration for certain luminaire characteristics such as beam width and non-luminous separation between individual sources. Depending on these factors, certain norms can suggest LPD limits much larger than required, or too small inducing measurement errors particularly in off-axis directions. Therefore, the search for updated standard measurement distances is advised.

Acknowledgements

We thank Tony Bergen and Lambert Tissot from the Australian Photometry and Radiometry Laboratory for their help in gathering of the measurement data used for the model validation. We also thank Johannes Ledig from the Physikalisch-Technische Bundesanstalt for the insights gained regarding the influence of the projected centre of gravity.

References

- ANSI/IES 2019. ANSI/IES LM-79-19. Approved Method: Optical and Electrical Measurements of Solid State Lighting Products. New York: 2019.
- BERGEN, A.S.J., and JENKINS, S.E. 2012. Determining the Minimum Test Distance in the Goniophotometry of LED Luminaires. In: *Proceedings of CIE 2012 Lighting Quality & Energy Efficiency, 19 - 21 September, Hangzhou, China*. Vienna: CIE, 337–343.
- CAI, W., LIU, X., ZHANG, P. and CHEN, W. 2013. Analysis of far-field distance of LED arrays based on an improved error calculation formula. In: *Proceedings SPIE: Nonimaging Optics: Efficient Design for Illumination and Solar Concentration X. Volume 8834*. <https://doi.org/10.1117/12.2022417>.
- CIE 1979. CIE 43:1979. Photometry of floodlights. Vienna: CIE.
- CIE 2015. CIE S 025/E:2015. Test Method for LED Lamps, LED Luminaires and LED Modules. Vienna: CIE.
- CIE 1996. CIE 121-1996. The photometry & goniophotometry of luminaires. Vienna: CIE
- DOTREPPE, G., AUDENAERT, J., SCHEIR, G., VAN DAN BOSSCHE, P. and JACOBS, V.A.J., 2023. Off-axis limiting photometric distance of Lambertians and narrow beams. *Lighting Research & Technology*, 56(6), 550-569. <https://doi.org/10.1177/14771535231208933>.
- IEC 2010. IEC/TR 61341:2010. Method of measurement of centre beam intensity and beam angle(s) of reflector lamps. Geneva: IEC.
- JACOBS, V., FORMENT, S., ROMBAUTS, P., HANSELAER, P. 2014. Near-field and far-field goniophotometry of narrow-beam LED arrays. *Lighting Research and Technology*, 47(4), 470-482. <https://doi.org/10.1177/1477153514530139>
- JACOBS, V., BLATTNER, P., OHNO, Y., BERGEN, T., KRUEGER, U., HANSELAER, P., ROMBAUTS, P., & SCHMIDT, F. 2015. Analyses of errors associated with photometric distance in goniophotometry. In: *Proceedings of the 28th Session of CIE, June 28 – July 4, Manchester, United Kingdom*.
- LIU, X., CAI, W., LEI, X., DU, X., CHEN, W. 2013. Far-field distance for surface light source with different luminous area. *Applied Optics*, 52(8): 1629. <https://doi.org/10.1364/AO.52.001629>.
- MORENO, I., AND SUN, C.-C. 2008. LED array: Where does far-field begin? In: *Proceedings SPIE 7058, Eighth International Conference on Solid State Lighting, 2 September 2008, San Diego, California, United States*. <https://doi.org/10.1117/12.795944>.
- MORENO, I., SUN, C.-C. AND IVANOV, R. 2009. Far-field condition for light-emitting diode arrays. *Applied Optics*, 48(6), 1190–1197. <https://doi.org/10.1364/AO.48.001190>.
- SIMONS, R. and BEAN, A. 2001. *Lighting Engineering: Applied Calculations*. London: Routledge
- SUN, C.-C., CHIEN, W.-T., MORENO, I., HSIEH, C.-C., and LO, Y.-C. 2009. Analysis of the far-field region of LEDs. *Optics Express*, 17(16), 13918–13927. <https://doi.org/10.1364/OE.17.013918>.
- SUN, C. C., LIN, Y. S., YANG, T. H., LIN, S. K., LEE, X. H. WU, C. S. AND YU, Y. W. 2020. Illuminance and starting distance of the far field of LED-array luminaire operated at short working distance. *Crystals*, 10(5). <https://doi.org/10.3390/cryst10050360>.